THE JOURNAL OF PHYSICAL CHEMISTRY B

ARTICLE

pubs.acs.org/JPCB

Sequence-Dependent pK_a Shift Induced by Molecular Self-Assembly: Insights from Computer Simulation

Jagannath Mondal, Xiao Zhu, Qiang Cui, and Arun Yethiraj*

Department of Chemistry, University of Wisconsin, Madison, Wisconsin 53706, United States

Supporting Information

ABSTRACT: The control of catalytic activity using molecular self-assembly is of fundamental interest. Recent experiments (Muller et al., *Angew. Chem., Int. Ed.*, **2009**, *48*, 922−925) have demonstrated that two sequence isomers of β-peptides show remarkably different activity as an amine catalyst for a retro-aldol cleavage reaction, a difference attributed to the ability of one of the sequences to form large aggregates. The self-assembly and catalytic activity of these two isomers are investigated using constant pH molecular dynamics (CPHMD), for an atomistic model of β-peptides in implicit solvent. Simulations show that the globally amphiphilic (GA) isomer, which experimentally has high activity, forms large aggregates, while the non-GA isomer forms aggregates that are at most three or four molecules in size. The pK_a shift of the βK-residues is significantly higher in the GA isomers that make a large aggregate. Since the decrease in pK_a of the side-chain ammonium group is the main driving force for amine catalysis, the calculations are consistent with experiment. We find that the buried βK residues become entirely deprotonated, and the pK_a shift for other titratable βK residues is accompanied *mainly* by a clustering of solvent exposed βK residues. We conclude that simulations can be used to understand catalytic activity due to self-assembly.

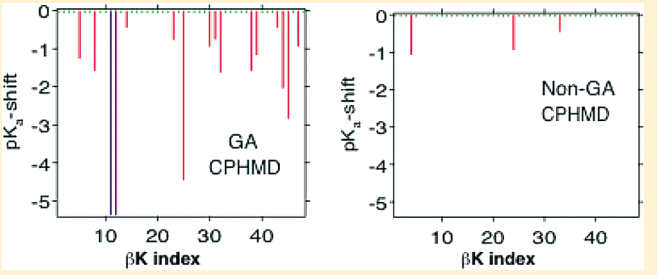

1. INTRODUCTION

An important direction in nanotechnology is the fabrication of functional nanomaterials. The past decade has seen significant advances in the bottom-up fabrication of self-assembled structures, and incorporating function into these nanostructured materials is of interest. An example is the design of materials which possess catalytic activity when self-assembled, in which case a directed assembly can impart catalytic activity to a material.

An example of such a function was reported recently by Muller et al.[1] who showed that a class of materials made from β-peptide oligomers were efficient amine catalysts for the retroaldol cleavage reaction. The catalytic activity was strongly sequence dependent: sequences that are known to self-assemble into long hollow cylinders showed catalytic activity, and sequence isomers that do not self-assemble did not. In this work, we present theoretical calculations to provide physical insight into the sequence dependence of catalytic activity.

The molecules studied by Muller et al.[1] are oligomers of β-amino acids, which contain an additional carbon atom on the backbone when compared to natural amino acids. This allows the incorporation of cyclic groups along the backbone resulting in very stable helical structures.[3] The spatial arrangement of side groups can be controlled via the sequence of the molecules.[4,5] For example, for the β-peptide βY-(ACHC-ACHC-βK)$_3$ globally amphiphiic (GA) and non-GA sequence isomers can be constructed by changing the sequence of the residues, without altering the overall composition (see Figure 1). In the GA sequence, one of the three helical faces contains only hydrophilic residues, while the other two contain only hydrophobic residues. In the non-GA sequence, each of the three helical faces contains one hydrophilic and two hydrophobic residues. For these molecules (capped with a heptanoyl moiety in the N-terminus), they found that the GA sequence isomer was an efficient catalyst, but the non-GA sequence isomer was not.

In the reaction studied by Muller et al.,[1] catalytic activity can be correlated with the pK_a of the amine groups. In the retroaldol cleavage reaction they investigated, β-hydroxyketone is subjected to a C−C bond fission to produce benzaldehyde and pyruvate. The catalytic cycle is initiated by nucleophilic attack of an amine on the carbonyl group of the hydroxy-ketone to form an imine, and this imine formation is the rate-limiting step.[6] The catalytic activity is expected to increase with an enhancement in the nucleophilicity of the amine,[6−8] which can be achieved by an environment that lowers the pK_a of the amine groups. They observed an increase of catalytic activity by about an order of magnitude for the GA sequence which is consistent with a pK_a shift of 2−3 units. A similar correlation between catalytic activity and pK_a shift was reported by Lassilaa et al.[2] who studied the origin of catalysis in computationally designed retroaldolase enzymes. They reported a pK_a drop of lysine groups from 10.6 in solution to about 6.8−7.5 in the enzyme, which accounted for approximately an order of magnitude increase in catalytic activity.

Received: July 28, 2011
Revised: November 27, 2011
Published: November 28, 2011

ACS Publications © 2011 American Chemical Society

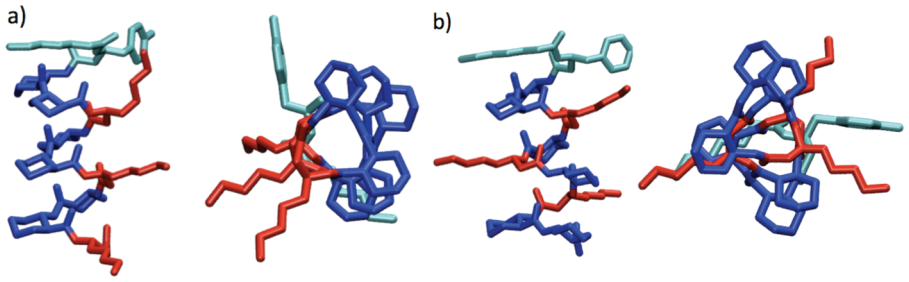

Figure 1. Top and side views of the (a) GA and (b) non-GA sequences of the experimentally studied β-peptide showing how the sequence imparts amphiphilicity. Color code: βK (red), ACHC (blue), βY and backbone atoms (cyan), where ACHC, βK, and βY refer to the cyclic residue *trans*-2 aminocyclohexane carboxylic acid and β^3-homolysine and β^3-homotyrosine, respectively. The chemical formula of these two isomers corresponds to that of peptide Nos. 2 and 3 in ref 1.

The connection between catalytic activity and self-assembly in the β-peptide oligomers is established by noting that the GA isomer self-assembles into long hollow cylinders, but the non-GA isomer does not.[9] It was hypothesized that the self-assembly altered the environment of the amine groups in the two sequences, resulting in different pK_a drops (compared to isolated molecules) in the sequence isomers.

To explicitly test this hypothesis, one needs to compare the apparent pK_a of the amine groups in the aggregates of the GA and non-GA isomers. An important question is whether the magnitude of the pK_a shift (thus presumably the sequence dependence of the catalytic activity) depends critically on the aggregates or is largely determined by the electrostatic properties of individual peptides. For this purpose, one popular computational approach is based on solving the Poisson−Boltzmann (PB) equation and comparing the electrostatic free energy of a biopolymer in different protonation states. Indeed, this protocol has been used extensively to calculate pK_a shifts in biological molecules. Bashford and Karplus[10] evaluated pK_a shifts of the ionizable groups in lysozyme and showed that the method reproduced most of the experimentally observed pK_a shifts. The method has also been used to provide insight on the functional role of salt bridges in proteins,[11] the pH-induced release of iron from transferrin,[12] the binding of calcium ions to proteins,[13] the electrostatic properties of bovine β-lactoglobulin,[14] and the functional role of titratable functional groups of several protein−enzyme complexes such as class A β-lactamases,[15] protein-tyrosine phosphatage,[16] methoxyrate-enzyme complexes,[17] and HIV-1 protease.[18] Recently, McCammon and co-workers[19] have calculated the electrostatic potentials for supramolecular structures such as the ribosome and microtubules.

However, there are two problematic issues with applying the PB method to the problem of interest here. The first is that the structure of the molecule does not adjust to the protonation state; the pK_a shift is calculated post facto. For proteins in the native state, this is not a major issue, but this could be a problem for the self-assembling systems of interest. For example, in the PB method large pK_a shifts will be predicted for residues buried within hydrophobic regions, but such a burial might not occur if the conformation is allowed to adjust to the protonation state or if the protonation state of a given site can change. The second issue is that the solute dielectric constant is an adjustable parameter in the PB calculation and must be manually (and somewhat arbitrarily) selected. Selecting this parameter is problematic because the dielectric constant can vary from 4 to 40 depending on the location.[20−25] Furthermore, this parameter plays a significant role in the calculated magnitude of the pK_a shift.

An alternative to the PB method is via a constant pH molecular dynamics (CPHMD) method[26−32] where protonation−deprotonation events are incorporated into the molecular dynamics simulation. We follow the method of Brooks and co-workers[30−32] where the set of titration coordinates is propagated along with the spatial coordinates in an implicit solvent framework. The conformations adjust to the titration state, and no choice of dielectric constant is necessary. The method has been extensively tested on protein titrations[32] and has been applied to study pH-dependent mechanisms of protein folding.[33−36]

In this work, we use atomistic models for the peptides and an implicit solvent to study the aggregation and pK_a shift for the two sequences. We calculate the pK_a shift using CPHMD simulations. Consistent with experiments, we find significant sequence dependence in pK_a shifts. We find that the pK_a shift for titratable βK residues is accompanied *mainly* by a clustering of βK residues. The βK residues that are buried (in CPHMD simulations) become entirely deprotonated and therefore no longer participate in proton equilibration.

The rest of this paper is organized as follows: the simulation model and methods are described in Section 2, results are presented in Section 3, and some conclusions are presented in Section 4.

2. SIMULATION MODEL AND METHODS

We study atomistic models of the GA and non-GA sequence isomers of the β-peptide βY-(ACHC-ACHC-βK)$_3$ (see Figure 1). (These molecules differ from the "Model A" molecules studied in our previous work[37−40] because of an additional hydrophobic tail at the N-terminus containing seven CH_2 groups.) For the β-peptides, we employ the atomistic force field developed by Zhu et al.,[41−43] which has parameters compatible with the CHARMM model[44] for solvent and natural amino acids, and we use the CHARM22 force field[44] for the hydrophobic tail.

We use constant pH molecular dynamics (CPHMD) simulations to calculate the pK_a shift of the ionizable lysine side chains. CPHMD simulations are carried out using the PHMD and GBSW modules within the CHARMM molecular dynamics program.[50] The theoretical background for this method is described by Brooks and co-workers.[30−32] The CPHMD method is an extended Hamiltonian approach, where a set of titration coordinates is propagated simultaneously with the spatial coordinates.

Since the explicit solvation of the entire system requires a prohibitive number of water molecules, the solvent is treated implicitly using the GBSW[45−49] (Generalized Born model with a SWitching function) implicit solvent model implemented in the

dx.doi.org/10.1021/jp2071953 |*J. Phys. Chem. B* 2012, 116, 491–495

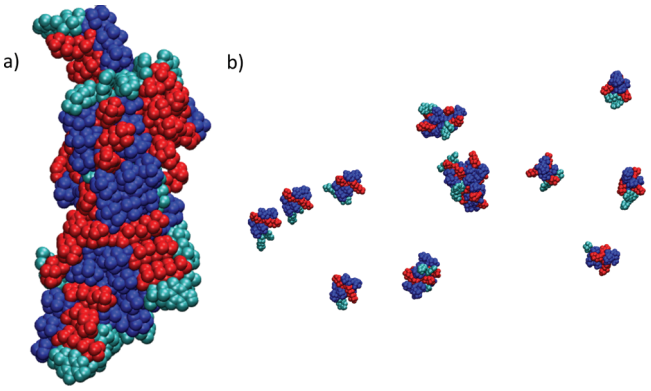

Figure 2. Representative snapshots (in space-filling representation) of aggregates for (a) GA sequence and (b) non-GA sequence obtained using the CPHMD method. Color code: βK (red), ACHC (blue), βY and acyl tail (cyan).

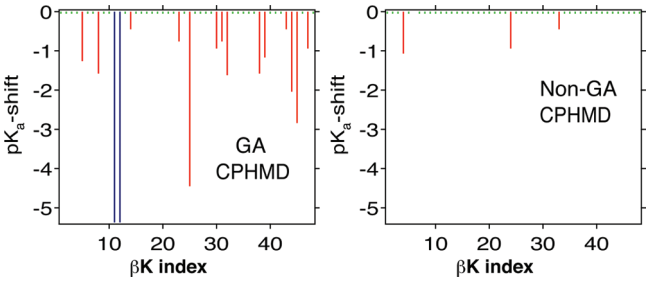

Figure 3. Comparison of pK_a shift between (a) GA sequence and (b) non-GA sequences of the β-peptide for each of the βK residues. Color code for the pK_a shift obtained using CPHMD: green lines correspond to βK sites with the fully deprotonated population <0.0001; blue lines correspond to βK sites with the fully deprotonated population >0.9999 (thus very large pK_a shift); red lines correspond to βK sites with the fully deprotonated population between 0.0001 and 0.9999.

CHARMM program.[50] The use of the GBSW implicit solvent model for β-peptides is justified by our recent simulation study[39] on the similar set of β-peptides: semiquantitative agreement was found between explicit and implicit solvent for the free energy of association of a pair of β-peptides. In accordance with experimental conditions,[1] we set the salt concentration to 150 mM using the method of Case and co-workers.[51] We use atomic radii optimized by Nina and co-workers[52,53] for the acyclic residues and obtain those for the side-chain carbon atoms of cyclic residues from that of proline. The hydrogen atomic radii are set to zero by convention. A dielectric switching length of 0.4 Å is used along with 50 Lededev angular integration points and 24 radial integration points up to 20 Å for each atom. The effective Born radii are updated every 2 time steps. The nonpolar contribution to the solvation free energy is estimated using the solvent-accessible surface area (SASA) model with a surface tension coefficient of 0.005 kcal/(mol Å^2). We use a 20 Å cutoff for the nonbonded interaction.

In accordance with the experimental pH,[1] a constant pH of 8 is maintained in the simulation. The initial configuration consists of 16 well-separated copies of molecules. For the 16 copies of β-peptides, there are 48 titration coordinates[30−32] (λ_i, i = 1, ..., 48), and we use the same parameter set for the β-lysine side chains as has been used for α-lysine side chains; i.e., the partial charges are the same as in α-lysine side chains, and the reference pK_a is 10.4.

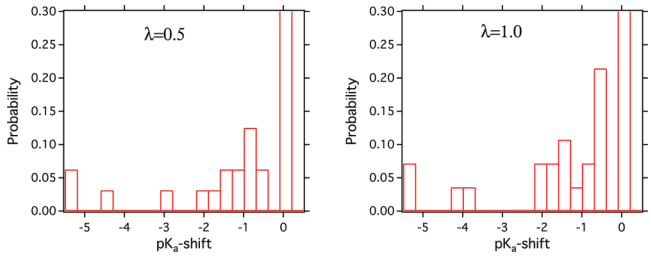

Figure 4. Comparison of population of pK_a shifts from CPHMD simulations with different starting λ values (with pH = 8). For convenience of visualization of higher pK_a shifts (greater than 0), the y-axis range has been reduced to 0.3.

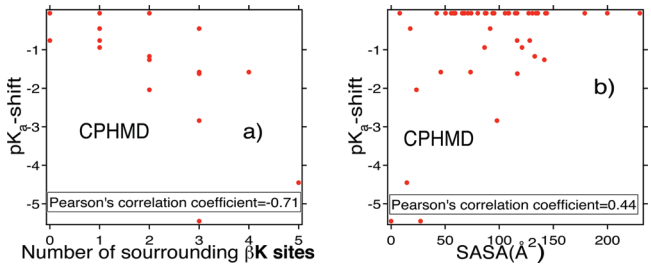

Figure 5. Correlation of pK_a shift with (a) number of surrounding βK residues and (b) SASA of the βK residues for the GA isomer obtained using the CPHMD simulation method. For sites with the fully deprotonated population >0.9999, which in principle have very large pK_a shifts, a value of ∼−5 is assigned for plotting purposes; these sites are also included in the Pearson correlation coefficient calculations. Note that many data points overlap in (a).

A titration barrier of 1.25 kcal/mol is used to suppress the fractional population of mixed titration states. The system is evolved using Langevin dynamics at 300 K for 40 ns with a time step of 2 fs and a friction coefficient of 5 ps^{-1} for the heavy atoms. All bonds to hydrogen atoms are constrained with SHAKE.[54] Five trajectories with different random velocity seeds are generated for both the sequence isomers.

To avoid bias, these first sets of simulations are started with λ_i = 0.5 for all sites. To test for convergence, additional simulations are carried out with the final configuration from the first set of simulations as the initial configuration, but all λ_i = 1 (i.e., all βK are fully unprotonated). These second sets of simulations contain five independent trajectories of 6 ns each.

We assign a state to be unprotonated if the titration coordinate value is more than 0.95 and protonated if the titration coordinate value is less than 0.05. Using the last few nanoseconds of the simulation trajectory, we first extract the fraction of unprotonated states (S^{unprot}) and from S^{unprot} calculate the pK_a of each site by solving the Henderson−Hesselbach (HH) equation (eq 1)

$$S^{\text{unprot}} = \frac{1}{1 + 10^{(\text{p}K_a - \text{pH})}} \quad (1)$$

The solvent accessible surface area and pK_a shift are calculated during the last 5 ns of the simulation. We calculate the SASA of each of the βK residues by rolling a water probe of radius 1.4 Å to quantify the burial of hydrophilic residues in a hydrophobic core. We also calculate the number of surrounding βK residues within a cutoff distance of 13 Å from a particular βK residue.

dx.doi.org/10.1021/jp2071953 |J. Phys. Chem. B 2012, 116, 491–495

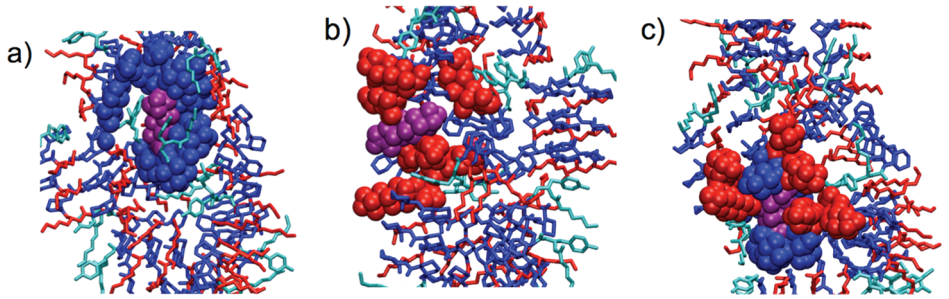

Figure 6. Representative snapshots from the CPHMD simulation emphasizing the different factors for the pK_a shift of βK sites (purple colored): (a) a βK site with a negligible pK_a shift due to a very small SASA but no clustering of other βK residues; (b) a βK residue with a significant pK_a shift due to a large SASA but an extensive clustering of βK residues; (c) a βK residue with a significant pK_a shift due to the cooperative effect of a small SASA along with an extensive clustering of βK residues. In all snapshots, the βK residue of interest is shown in purple; surrounding ACHC groups within 6 Å are shown in blue; and βK residues within 13 Å are shown in red using a space-filling representation. The rest of the aggregate is shown in a licorice representation.

All snapshots in this article are rendered using Visual Molecular Dynamics (VMD).[57]

3. RESULTS AND DISCUSSION

The self-assembly of the β peptides studied is strongly sequence dependent. Experimentally, the GA isomers form large aggregates, and the non-GA isomers do not.[9] We have previously investigated the self-assembly of these molecules using coarse-grained models[38] and potential of mean force calculations.[39] We found that the most favorable conformation for three molecules of the GA isomer is a side-to-side parallel arrangement with a slight curvature. This favors the formation of rings, which then stack to make tubes. Simulations starting with an unaggregated configuration of molecules did not form tubes, although they aggregated in a sequence-dependent fashion,[38] emphasizing the high barrier to tube formation. The simulations of this work with implicit solvent are consistent with previous calculations.

The two sequence isomers show distinct sequence dependence in the self-aggregation. Starting with a configuration of 16 copies of well-separated β-peptides, the GA sequence isomers self-assemble spontaneously to form a single large aggregate, while non-GA isomers form smaller globules consisting of at most 3−4 molecules, as depicted in the representative snapshots in Figure 2, with a radius of gyration of 21.0 ± 0.2 Å.

The difference in aggregation of molecules is accompanied by a significant difference in the pK_a shift of the ionizable βK groups between the two isomers. Figure 3 depicts the pK_a shift for each of the βK residues in the GA and non-GA sequences. As depicted in Figure 3, the βK residues in the GA isomer undergo systematically larger pK_a shifts than those in the non-GA isomer. Note that for an isolated β-peptide molecule the pK_a shifts of the three βK residues are very minor. For the GA isomer, the pK_a shifts of the three βK residues (starting from the N-terminus) are +0.17, −0.18, and −0.009, respectively, relative to the β amino acid. Furthermore, there is little difference between the isolated GA and non-GA isomers in solution (a maximum of only −0.12), which emphasizes that the pK_a shift observed in CPHMD simulations is an outcome of the sequence dependence in self-assembly. The qualitative trends do not depend significantly on the initial λ values (Figure 4).

On the basis of CPHMD results, βK sites can be categorized into three different types: a few of them remain fully protonated (fully unprotonated population <0.0001), some of them become fully deprotonated (fully deprotonated population >0.9999), while the rest remain partially protonated. Analysis of the results indicates that the pK_a shift arises mainly from a clustering of multiple βK residues. Figure 5 compares the number of surrounding βK sites (within a cutoff distance of 13 Å) with the corresponding pK_a shift of each of 48 lysine sites in the aggregate obtained using the CPHMD simulation technique. The significantly negative Pearson's correlation coefficient value of −0.71 between the number of surrounding lysine residues and the corresponding drop in pK_a reflects the general trend that residues with a larger number of surrounding lysine residues undergo a larger drop in pK_a. Although quite a few βK sites are buried in the hydrophobic core, there is a relatively low (0.44) correlation between the SASA value with pK_a shifts. Since a buried βK has a significant deprotonated population in the CPHMD simulations, this observation suggests that the interaction between the positively charged βK side chain and backbone likely drives the burial of βK despite the desolvation penalty.

Snapshots representing the above scenarios are shown in Figure 6. Figure 6a shows an instance of small pK_a shifts of isolated βK sites. The pK_a shift due to clustering is manifested either in the form of clustering of solvent-accessible βK sites (Figure 6b) or in the form of cooperative effect of small SASA and clustering of surrounding βK sites (Figure 6c). The fact that smaller SASA alone does not lead to a very large pK_a shift unless there is extensive clustering of βK residues is important for the catalytic activity because only solvent-accessible βK residues with low pK_a values are expected to be catalytically active.

4. CONCLUSIONS

We use atomistic simulations to rationalize the experimentally observed sequence dependence in pK_a shift and hence catalytic efficiency of two sequence isomers of a 14-helical amphiphilic β-peptide. We find that the sequence dependence in the catalytic activity can be explained by the difference in the pK_a shift, which in turn is dependent on the respective sequence-isomer's tendency to self-assemble into distinct structures. By contrast, negligible pK_a shifts are observed for both peptides in isolation. Therefore, our calculations have provided explicit evidence that links self-assembly behaviors and catalytic activities in these non-natural peptides.

Constant pH molecular dynamics simulation captures the sequence-dependent pK_a shift. Even though both a decrease in solvent accessible surface area and an increase in local charge density contribute to the pK_a shift, we attribute the pK_a shift *mainly*

to clustering of βK residues because highly buried βK residues tend to remain fully deprotonated. For a thorough description of self-assembly driven catalysis, an explicit consideration of protonation−deprotonation events is important, and therefore the CPHMD approach is preferable.

■ ASSOCIATED CONTENT

Supporting Information. Information on pK_a shift calculated using another method called the "static pK_a method" for the same two β-peptides, where the pK_a shifts of the ionizable residues are computed by first performing a conventional molecular dynamics method followed by a Poisson−Boltzmann electrostatic free energy calculation. The detailed method and comparison with results obtained using the CPHMD method are documented. This material is available free of charge via the Internet at http://pubs.acs.org.

■ AUTHOR INFORMATION

Corresponding Author
*E-mail: yethiraj@chem.wisc.edu.

■ ACKNOWLEDGMENT

This research was supported by the National Science foundation through the UW—Madison Nanoscale Science and Engineering Center (NSEC) (NSF grant DMR-0832760) and Grant No. CHE-0717569. We are grateful for computational support from Abe machine in National Center for Supercomputing Application (NCSA) under grant number TG-CHE090065 and the UW Madison Centre for High Throughput Computing (CHTC) Condor supercomputing facility. We thank Professor Sam Gellman and Dr. Matt Windsor for useful discussions. We thank Dr. Jason Wallace (in Professor Jana Shen's group) for useful discussions regarding the PHMD module in CHARMM.

■ REFERENCES

(1) Muller, M. M.; Windsor, M. A.; Pomerantz, W. C.; Gellman, S. H.; Hilvert, D. *Angew. Chem., Int. Ed.* **2009**, *48*, 922.
(2) Lassila, J. K.; Baker, D.; Herschlag, D. *Proc. Natl. Acad. Sci.* **2010**, *107*, 4937.
(3) Cheng, R. P.; Gellman, S. H.; Degrado, W. F. *Chem. Rev.* **2001**, *101*, 3219.
(4) Gellman, S. H. *Acc. Chem. Res.* **1998**, *31*, 173.
(5) Horne, W. S.; Gellman, S. H. *Acc. Chem. Res.* **2008**, *41*, 1399.
(6) Johnson, K.; Alleman, R. K.; Widmer, H.; Benner, S. A. *Nature* **1993**, *365*, 530.
(7) Tanaka, F.; Fuller, R.; Barbas, C., III *Biochemistry* **2005**, *44*, 7583.
(8) Weston, C. J.; Cureton, C. H.; Calvert, M. J.; Smart, O.; Alleman, R. K. *ChemBioChem* **2004**, *5*, 1075.
(9) Pomerantz, W. C.; Abbott, N. L.; Gellman, S. H. *J. Am. Chem. Soc.* **2006**, *128*, 8730.
(10) Bashford, D.; Karplus, M. *Biochemistry* **1990**, *29*, 10219.
(11) Lounas, V.; R., W. *Biochemistry* **1997**, *36*, 5402.
(12) Lee, D. L.; Goodfellow, J. M. *Biophys. J.* **1998**, *74*, 2747.
(13) Penfold, R.; Warwicker, J.; Jönsson, B. *J. Phys. Chem. B* **1998**, *102*, 8599.
(14) Fogolari, F.; Ragona, L.; Licciardi, S.; Romagnoli, S.; Michelutti, R.; Ugolini, R.; Molinari, H. *Proteins: Struct., Funct., Genet.* **2000**, *39*, 317.
(15) Raquet, X.; ad Lounnas, V.; Frere, J. M.; Wade, R. C. *Biophys. J.* **1997**, *73*, 2416.
(16) Peters, G. H.; Frimurer, T. M.; Olsen, O. M. *Biochemistry* **1998**, *37*, 5383.
(17) Cannon, W.; Garrison, B. R.; Benkovic, S. J. *J. Mol. Biol.* **1997**, *271*, 656.
(18) Trylska, J.; Antosiewicz, J.; Geller, M.; Hodge, C.; Klabe, R. M.; Head, M. S.; Gilson, M. K. *Protein Sci.* **1999**, *8*, 180.
(19) Baker, N. A.; Sept, D.; Joseph, S.; Holst, M. J.; Mccammon, J. A. *Proc. Natl. Acad. Sci. U.S.A.* **2001**, *98*, 10037.
(20) Antosiewicz, J.; McCammon, J. A.; Gilson, M. K. *J. Mol. Biol.* **1994**, *238*, 415.
(21) Antosiewicz, J.; McCammon, J. A.; Gilson, M. K. *Biochemistry* **1996**, *35*, 7819.
(22) Sham, Y.; Chu, Z. T.; Warshel, A. *J. Phys. Chem. B* **1997**, *101*, 4458.
(23) Simonson, T.; Brooks, C. L., III *J. Am. Chem. Soc.* **1996**, *118*, 8452.
(24) Schutz, C. N.; Warshel, A. *Proteins* **2001**, *44*, 400.
(25) King, G.; Lee, F. S.; Warshel, A. *J. Chem. Phys.* **1991**, *95*, 4366.
(26) Baptista, A.; Martel, P. J.; Petersen, S. B. *Proteins* **1997**, *27*, 523.
(27) Baptista, A.; Teixeira, V. H.; Soares, C. M. *J. Chem. Phys.* **2002**, *117*, 4184.
(28) Bürgi, R.; Kollman, P. A.; van Gunsteren, W. F. *Proteins* **2002**, *47*, 4184.
(29) Borjensson, U.; Huenberger, P. H. *J. Chem. Phys.* **2001**, *114*, 9706.
(30) Lee, M. S.; Salsbury, F., Jr.; Brooks, C., III *Proteins: Struct., Funct., Bioinf.* **2004**, *56*, 738.
(31) Khandogin, J.; Brooks, C., III *Biophys. J.* **2005**, *89*, 141.
(32) Khandogin, J.; Brooks, C., III *Biochemistry* **2006**, *45*, 9363.
(33) Khandogin, J.; Brooks, C., III *Annu. Rep. Comput. Chem.* **2007**, *3*, 13.
(34) Khandogin, J.; Brooks, C., III *Proc. Natl. Acad. Sci. U.S.A.* **2007**, *104*, 16880.
(35) Khandogin, J.; Chen, J.; Brooks, C., III *Proc. Natl. Acad. Sci. U.S.A.* **2006**, *103*, 18546.
(36) Khandogin, J.; Raleigh, D. P.; Brooks, C., III *J. Am. Chem. Soc.* **2007**, *129*, 3056.
(37) Mondal, J.; Sung, B. J.; Yethiraj, A. *J. Phys. Chem. B* **2009**, *113*, 9379.
(38) Mondal, J.; Sung, B. J.; Yethiraj, A. *J. Chem. Phys.* **2010**, *132*, 065103.
(39) Mondal, J.; Zhu, X.; Cui, Q.; Yethiraj, A. *J. Phys. Chem. C* **2010**, *114*, 13551.
(40) Mondal, J.; Zhu, X.; Cui, Q.; Yethiraj, A. *J. Phys. Chem. B* **2010**, *114*, 13585.
(41) Zhu, X.; Yethiraj, A.; Cui, Q. *J. Chem. Theort Comput.* **2007**, *3*, 1538.
(42) Zhu, X.; Konig, P.; Gellman, S. H.; Yethiraj, A.; Cui, Q. *J. Phys. Chem. B* **2008**, *112*, 5439.
(43) Zhu, X.; Konig, P.; Hoffmann, M.; Yethiraj, A.; Cui, Q. *J. Comput. Chem.* **2010**, *31*, 2063.
(44) MacKerell, A. D.; et al. *J. Phys. Chem. B* **1998**, *102*, 3586–3616.
(45) Im, W.; Lee, M. S.; Brooks, C. L., III *J. Comput. Chem.* **2003**, *24*, 1691.
(46) Feig, M. *Methods Biol.* **2008**, *443*, 181.
(47) Im, W.; Feig, M.; Brooks, C. L., III *Biophys. J.* **2003**, *85*, 2900.
(48) Im, W.; Brooks, C. L., III *Proc. Natl. Acad. Sci.* **2005**, *102*, 6771.
(49) Chen, J. H.; Im, W.; Brooks, C. L., III *J. Am. Chem. Soc.* **2006**, *128*, 3728.
(50) Brooks, B. R.; Bruccoleri, R. E.; Olafson, D.; States, J.; Swaminathan, S.; Karplus, M. *J. Comput. Chem.* **1983**, *4*, 187.
(51) Srinivasan, J.; Trevathan, M. W.; Beroza, P.; Case, D. A. *Theor. Chem. Acc.* **1999**, *426*, 101.
(52) Nina, M.; Beglov, D.; Roux, B. *J. Phys. Chem. B* **1997**, *101*, 5239.
(53) Nina, M.; Im, W.; Roux, B. *Biophys. Chem.* **1999**, *78*, 89.
(54) Ryckaert, J. P.; Ciccotti, G.; Berendsen, H. J. C. *J. Comput. Phys.* **1977**, *23*, 327.
(55) Im, W.; Beglov, D.; Roux, B. *Comput. Phys. Commun.* **1998**, *111*, 59.
(56) Gilson, M. K.; Sharp, K.; Honig, B. *J. Comput. Chem.* **1987**, *9*, 327.
(57) Humphrey, W.; Dalke, A.; Schulten, K. *J. Mol. Graphics* **1996**, *14*, 33–38.